DOI: 10.1111/nyas.14881

CONCISE REPORT

ANNALS OF THE NEW YORK ACADEMY OF SCIENCES

Tight junction formation by a claudin mutant lacking the COOH-terminal PDZ domain-binding motif

Sachiko Fujiwara[1,2] | Thanh Phuong Nguyen[1,2] | Kyoko Furuse[1] | Yugo Fukazawa[3,4] | Tetsuhisa Otani[1,2] | Mikio Furuse[1,2,5]

[1]Division of Cell Structure, National Institute for Physiological Sciences, Okazaki, Japan

[2]Department of Physiological Sciences, School of Life Science, SOKENDAI, The Graduate University for Advanced Studies, Okazaki, Japan

[3]Division of Brain Structure and Function, Faculty of Medical Sciences, University of Fukui, Fukui, Japan

[4]Life Science Innovation Center, University of Fukui, Fukui, Japan

[5]Nagoya University Graduate School of Medicine, Aichi, Japan

Correspondence
Mikio Furuse, Division of Cell Structure, National Institute for Physiological Sciences, 5-1 Higashiyama, Myodaiji, Okazaki, Aichi 444–8787, Japan.
Email: furuse@nips.ac.jp

Funding information
Japan Society for the Promotion of Science; Grant-in-Aid for Challenging Exploratory Research/16K15226; Grant-in-Aid for Scientific Research on Innovative Areas—Platforms for Advanced Technologies and Research Resources "Advanced Bioimaging Support"/16H06280; Grant-in-Aid for Scientific Research(B)/21H02523

Sachiko Fujiwara, Thanh Phuong Nguyen, and Kyoko Furuse contributed equally to this work.

Abstract

Claudin-based tight junctions (TJs) are formed at the most apical part of cell–cell contacts in epithelial cells. Previous studies suggest that scaffolding proteins ZO-1 and ZO-2 (ZO proteins) determine the location of TJs by interacting with claudins, but this idea is not conclusive. To address the role of the ZO proteins binding to claudins at TJs, a COOH-terminal PDZ domain binding motif-deleted claudin-3 mutant, which lacks the ZO protein binding, was stably expressed in claudin-deficient MDCK cells. The COOH-terminus-deleted claudin-3 was localized at the apicolateral region similar to full-length claudin-3. Consistently, freeze-fracture electron microscopy revealed that the COOH-terminus-deleted claudin-3-expressing cells reconstituted belts of TJs at the most apical region of the lateral membrane and restored functional epithelial barriers. These results suggest that the interaction of claudins with ZO proteins is not a prerequisite for TJ formation at the most apical part of cell–cell contacts.

KEYWORDS
claudin, PDZ domain-binding motif, tight junction, ZO-1

INTRODUCTION

Tight junctions (TJs) contribute to epithelial barrier function by regulating the passage of solutes via the intercellular space in vertebrate epithelial cells.[1–4] Among several types of TJ-associated membrane proteins, the claudin family constitutes the backbone of TJ structures. Claudins polymerize into a fibril-like structure within the plasma membrane, namely a TJ strand, which is visualized by freeze-fracture replica electron microscopy as a functional unit of TJs.[5] TJ strands attach to one another between adjacent cells to make a focal

membrane contact that can be visualized via ultrathin-section electron microscopy.[6,7] A network of claudin-based TJ strands surrounds the cell as a belt at the most apical region of the lateral membrane.[8] In most epithelial cell types, TJ strands consist of multiple claudin subtypes, each of which has its unique function in the barrier property of TJs.[9] Claudins have a PDZ domain-binding motif (PBM) at their COOH-termini and bind to the PDZ1 domain of ZO-1, ZO-2, and ZO-3 TJ-plaque proteins (collectively referred to as ZO proteins). Each ZO protein has three PDZ domains.[10] ZO proteins are thought to work as scaffolds for the assembly of membrane proteins, plaque proteins, signaling molecules, and actin cytoskeletons at TJs.[11]

One of the characteristic features of TJs is that they are formed at the most apical part of cell–cell contacts.[12] Although the detailed mechanism for the localization of TJ formation remains elusive, it has been demonstrated that ZO-1 and ZO-2 are required for TJ formation. EpH4 mammary epithelial cells in which ZO-1 and ZO-2 were deleted by homologous recombination and RNA interference, respectively, maintained epithelial polarity but lacked TJs, while the EpH4 cells lacking either ZO-1 or ZO-2 retained TJs.[13] Furthermore, claudins were polymerized to form TJ strands when the N-terminal half of ZO-1 containing three PDZ domains were forcibly recruited to the lateral membrane and dimerized in ZO-1 and ZO-2-deleted EpH4 cells.[13] Based on these observations, it has been proposed that ZO-1 and ZO-2 determine the location of TJs by interacting with claudins. MDCK II cells lacking both ZO-1 and ZO-2 (ZO-1/ZO-2 dKO cells) by genome editing primarily lacked TJs, while MDCK II cells lacking either ZO-1 or ZO-2 maintained TJs. These findings confirmed that both ZO-1 and ZO-2 are required for TJ formation.[14] However, ZO-1/ZO-2 dKO cells showed additional abnormalities in cell polarity, actomyosin organization, and cell–cell junction organization, which suggests ZO-1 and ZO-2 have multiple roles in the organization of epithelial cells.[14] Thus, the lack of TJ formation in ZO-1/ZO-2 dKO cells cannot solely be attributed to the loss of claudins interacting with ZO-1 or ZO-2.

Analyses of the behavior of a claudin mutant protein lacking the PBM in cultured cells provide an opportunity to clarify the role of claudins-ZO proteins binding in determinating the site of TJ formation. In nonpolarized mouse L fibroblasts, exogenous expression of claudin-1 and claudin-2 with COOH-terminal epitope tags, which should mask the PBM, and claudin-1 lacking most of its COOH-terminal cytoplasmic domain reconstituted TJ strand-like structures at cell–cell contacts.[5,6] Furthermore, COOH-terminal tagged claudin-1 and claudin-2 were localized at TJs at the apicolateral region of cell–cell contacts in MDCK cells that expressed these proteins.[15] These observations suggest that claudins can form TJs at the correct location in epithelial cells without interacting with ZO proteins. However, it is still possible that claudins lacking ZO proteins-binding are recruited to TJs by their interaction with TJ-forming endogenous claudins.

In this study, we address the role of the binding of claudins to ZO proteins in TJ formation at the apicolateral region of the plasma membrane. Compared to previous studies, we used TJ-deficient claudin quintuple KO MDCK II cells (claudin quinKO cells), which were generated from MDCK II cells by disrupting the genes of claudin-1, claudin-2, claudin-3, claudin-4, and claudin-7 via genome editing.[14] It is expected that exogenous expression of a certain claudin subtype in claudin quinKO cells would reconstitute TJs. We, therefore, introduced mouse claudin-3 or its mutant lacking the PBM into claudin quinKO cells. Stable transfectants were obtained, and the reconstituted TJs were analyzed.

MATERIALS AND METHODS

Cells and antibodies

MDCK II cells derived from canine kidney were provided by Masayuki Murata (Tokyo Institute of Technology). Claudin quinKO cells were established and characterized as described previously.[14] Cells were cultured in Dulbecco's modified Eagle's medium (#05919; Nissui) supplemented with 10% fetal calf serum. The following antibodies were used in this study: rabbit polyclonal anti-claudin-3 (#34-1700; Thermo Fisher Scientific), mouse monoclonal anti-FLAG (#014-22383; WAKO), rat monoclonal anti-occludin (clone MOC37),[16] mouse monoclonal anti-ZO-1(T8-754),[17] rat monoclonal anti-ZO-1(R26.4C),[18] rabbit polyclonal anti-myosin heavy chain IIB (#909901; BioLegend), mouse monoclonal anti-HA (Clone 3F10, #1186742300; Merck), rabbit polyclonal anti-GFP (#A-11122; Thermo Fisher Scientific), and mouse monoclonal anti-α-tubulin (Clone DM1A, #62204; Thermo Fisher Scientific). The following secondary antibodies were used: donkey anti-mouse IgG Alexa Fluor 405–conjugated (#A48257; Thermo Fisher Scientific), donkey anti-mouse IgG Alexa Fluor 488–conjugated (#A21202; Thermo Fisher Scientific), donkey anti-rabbit IgG Alexa Fluor 488–conjugated (#A21206; Thermo Fisher Scientific), donkey anti-rat IgG Cy3-conjugated (#712-165-153; Jackson ImmunoResearch Laboratories), and donkey anti-rabbit IgG Cy3-conjugated (#711-165- 152; Jackson ImmunoResearch Laboratories). F-actin was labeled with Alexa-488-phalloidin (#A12379; Thermo Fisher Scientific).

Establishment of stable transfectants

Mammalian expression plasmids for mouse claudin-3 and claudin-3ΔYVF containing a neomycin-resistant gene were constructed as described previously.[6,19] Claudin quinKO cells cultured on 35 mm dishes were transfected with the expression plasmids by lipofection using Lipofectamine® LTX Reagent with Plus Reagent (#15338100; Thermo Fisher Scientific) according to the manufacturer's instruction. After ∼12 days of selection with media containing 300 μg/ml of G418 (#09380-44; Nacalai Tesque), proliferated cell colonies were picked up as stable transfectant clones. The expression of claudin-3 and claudin-3ΔYVF in these cell clones were screened by immunofluorescence staining with the anti-claudin-3 and anti-FLAG antibodies, respectively.

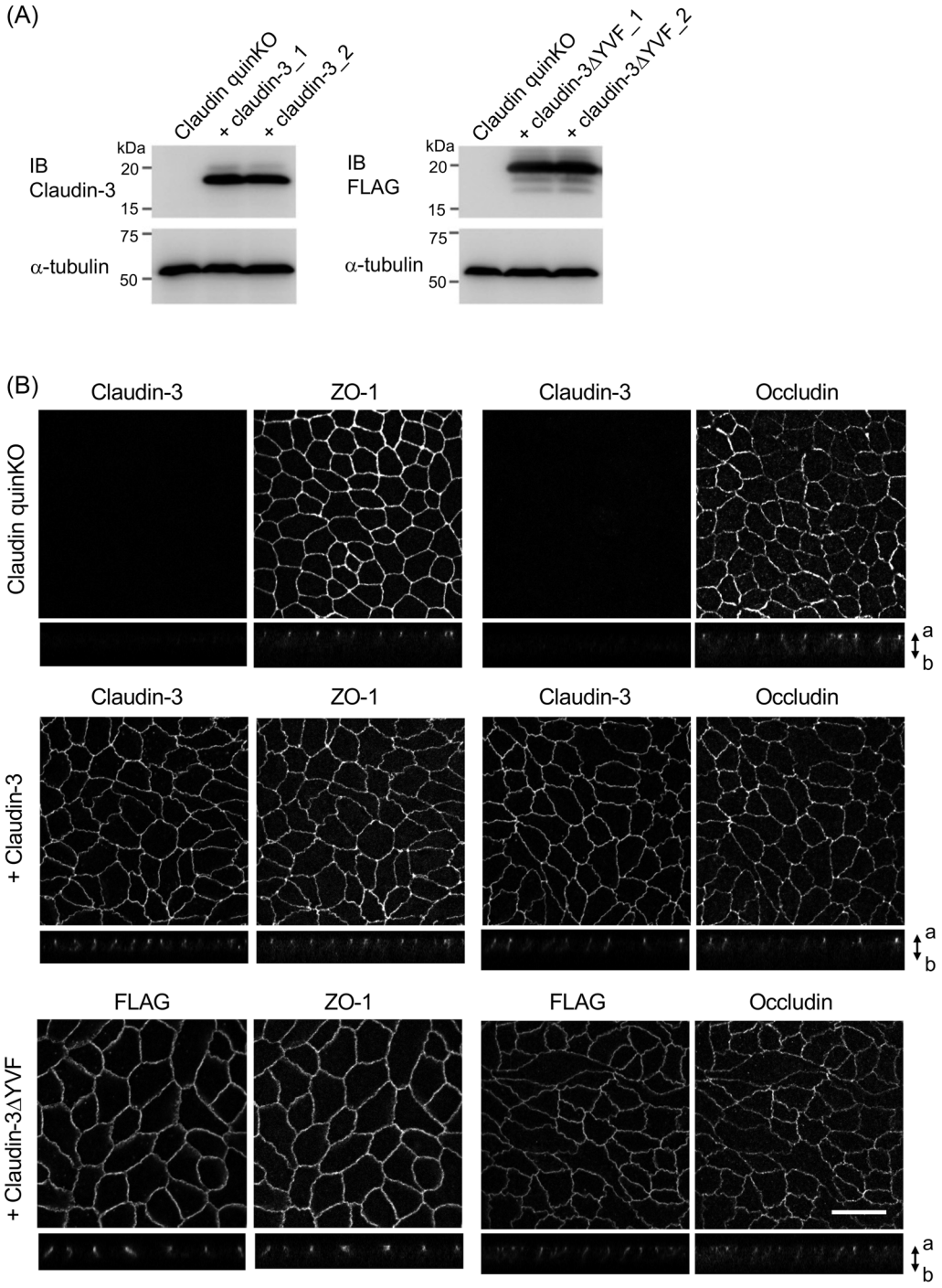

FIGURE 1 Expression and localization of exogenous claudin-3 and claudin-3ΔYVF in claudin quinKO cells. (A) Western blots of claudin quinKO cells, two clones of claudin-3-expressing cells, and two clones of claudin-3ΔYVF-expressing cells with anti-claudin-3 antibody, anti-FLAG antibody, or anti-α-tubulin antibody. (B) (Top panel) Immunofluorescence staining of claudin quinKO cells showed claudin-3 is absent, while ZO-1 and occludin strictly localize at apical cell–cell contacts. (Middle panel) Claudin-3-expressing cells clone 2 (+ Claudin-3) double-stained with anti-claudin-3 and anti-ZO-1 or anti-claudin-3 and anti-occludin. Claudin-3 is present along the lateral membrane and colocalized with ZO-1 and occludin at apical cell–cell contacts. (Bottom panel) Claudin-3ΔYVF-expressing cells clone 2 (+ Claudin-3ΔYVF) double-stained with anti-FLAG and anti-ZO-1 or anti-FLAG and anti-occludin antibodies. FLAG signals, which represent claudin-3ΔYVF, located along the lateral membrane and colocalized with ZO-1 and occludin at apical cell–cell contacts. The orthogonal views are shown below each image for the z-stack distribution; a and b with arrows represent apical and basal, respectively. Scale bar 20 μm.

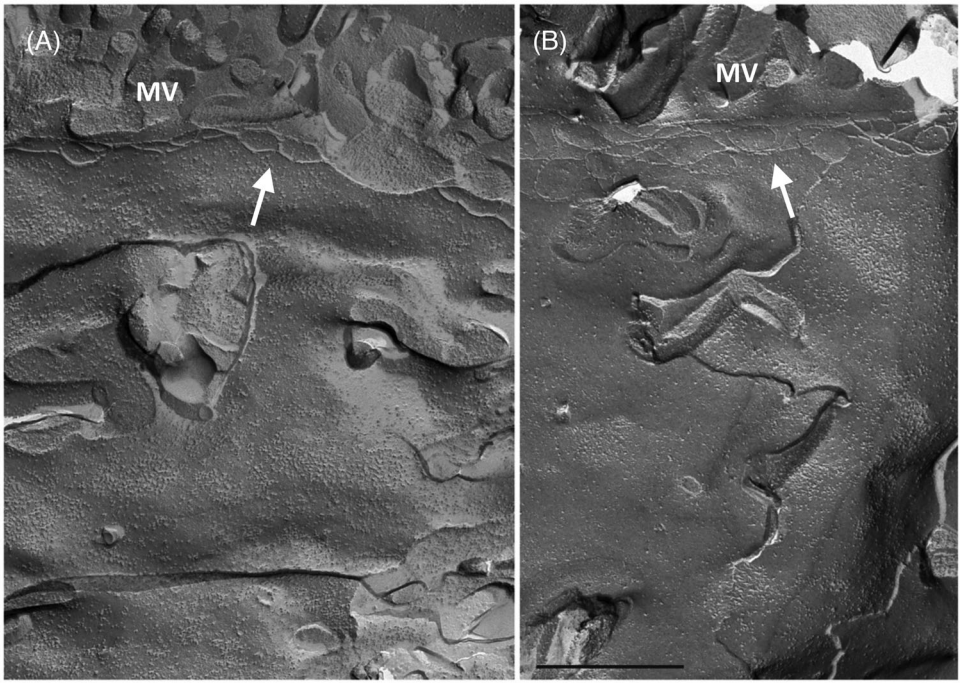

FIGURE 2 TJ strands reconstituted in claudin-3-expressing cells. (A, B) Two independent freeze-fracture replica images of claudin-3-expressing cells. Continuous belts of TJ strands are observed at the most apical region of the lateral membrane (arrows). MV, microvilli. Scale bar: 500 nm.

Immunoblotting

Cells were lysed with Laemmli SDS sample buffer supplemented with 100 mM DTT and boiled at 100°C for 5 min. The proteins were separated by SDS-PAGE using a 5% or 12.5% polyacrylamide gel. The proteins in the gels were transferred to PVDF membrane with 0.45 μm pore size (Millipore). The membrane was blocked with 5% skim milk in Tris-buffered saline supplemented with 0.1% Tween 20 (TBS-T) and incubated with primary antibodies diluted with 5% skim milk in TBS-T at room temperature for 30 min to 2 h or at 4°C overnight. The bound primary antibodies were detected using HRP-linked secondary antibodies and enhanced chemiluminescence (ECL prime; GE Healthcare). Images were obtained using LAS3000 Imager (Fujifilm).

Immunofluorescence staining

For immunofluorescence staining, cells were plated on Transwell polycarbonate membrane filters (12 well-pate; 0.4 μm pore size; 12 mm diameter insert; #3401; Corning) with 1×10^5 cells/well and cultured for 6 days with a medium change every 2 days. After removing the culture medium on day 6, cells were fixed with 10% TCA dissolved in distilled water for 30 min on ice.[20] For double staining of F-actin and myosin IIB, cells were fixed with 2% paraformaldehyde for 20 min at room temperature. Cells were washed with PBS three times, then permeabilized with 0.2% Triton X-100/PBS for 15 min at room temperature. All of the following procedures were conducted at room temperature. After permeabilization, the filters were cut in half to probe with different antibodies. Filter fragments were blocked with 10% FBS/PBS for 15 min. Cells were incubated with the primary antibodies for 1 h, washed with PBS three times, and incubated with the secondary antibodies for 1 h. After the secondary antibody incubation, cells were washed with PBS three times and mounted with FluorSave™ Reagent (#345789; Calbiochem®).

We obtained confocal images using a laser scanning confocal microscope. TCS-SPE was mounted on DMI 4000B and TCS-SP8 was mounted in DMI 6000CS using three laser lines (405/488/532 nm) and an objective lens of HCX PL APO 63×/NA 1.40 (Leica Microsystems). Confocal images were obtained using LAS-AF software. Samples were scanned with the z-step interval of 0.5 μm and 3× frames averaging was applied for each slice to obtain images in Figure 1B–D, and the z-step interval of 0.2 μm without averaging was used to obtain images in Figure 5. Images were analyzed using Fiji/ImageJ software version 2.3.0/1.53f. Original images were used to generate stacked images, and images shown in Figure 1B and Figure 5 were substacked from the apical region. The background was subtracted with a rolling ball radius of 50.0 pixels, and the brightness/contrast was adjusted.

Freeze-fracture replica electron microscopy

Except for some modifications in cell culture conditions, freeze-fracture replicas were produced using a method described previously.[21] The cells were plated and cultured on Transwell polycarbonate membrane filters (#3401; Corning) in the same conditions

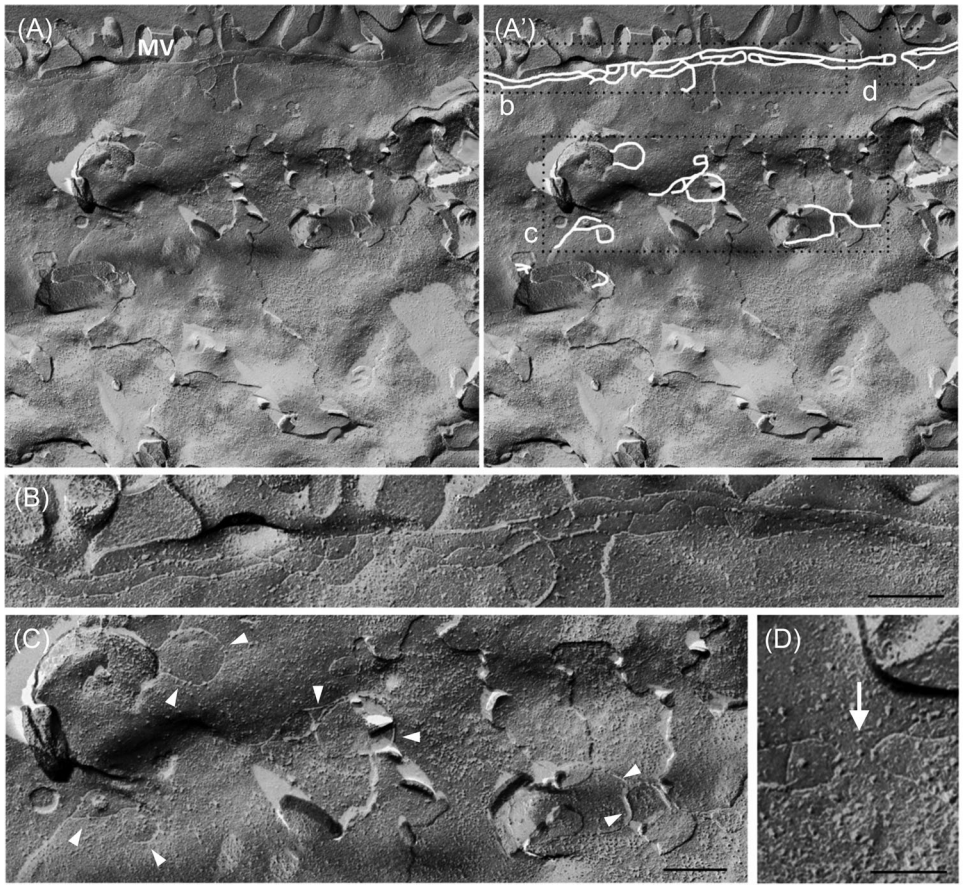

FIGURE 3 TJ strands reconstituted in claudin-3ΔYVF-expressing cells. (A) Freeze-fracture replica of claudin-3ΔYVF-expressing cells. (A') TJ strands in (A) are traced in white. Dotted rectangles (b), (c), and (d) are enlarged in (B), (C), and (D), respectively to clearly show TJ strands. TJ strands are reconstituted at the most apical region of the lateral membrane close to microvilli (MV) (B, C). (C) Fragmented TJ strands are observed in the lateral membrane (arrowheads). (D) Discontinuity of apical TJ strands (arrow). Scale bars: 500 nm in A'; 200 nm in B and C; 100 nm in D.

used for immunofluorescence staining. After 6 days of culture, cells were fixed with 2% glutaraldehyde in 0.1 M phosphate buffer (PB), pH 7.4, at 4°C overnight. The fixed cells were removed from the filters with scalpels, cryoprotected with 30% glycerol in 0.1 M PB at 4°C overnight, and then rapidly frozen in between two copper carriers by using a high-pressure freezing machine (HPM010, BAL-TEC, Balzers, Liechtenstein). The cells were fractured by separating the two carriers at −120°C and then replicated by platinum (45° unidirectional from horizontal level, 2 nm thick) and carbon (20 nm thick) in a freeze-fracture replica machine (BAF060, BAL-TEC). The replicated materials were transferred to glass vials filled with a solution containing kitchen bleach (50%) and incubated on a reciprocal shaker until cell debris was removed from the replicas. The replicas were washed twice with distilled water and transferred to grids coated with pioloform (Agar Scientific, Stansted, Essex, UK) for transmission electron microscope observation. The samples were observed with a JEM1010 transmission EM (JEOL, Tokyo, Japan) at 100 kV accelerating voltage. Images were captured with a Veleta CCD camera using iTEM software (Olympus Soft Imaging Solutions). Cell–cell junctions at the most apical cell contacts were observed.

Transepithelial electrical resistance and paracellular tracer flux

Cells at a concentration of 1×10^5 were seeded on 12 mm diameter Transwell polycarbonate filters with a 0.4 μm pore size (#3401, Corning). At 4 days of culture, the medium was changed to phenol-red free DMEM (08459-45; Nacalai Tesque) supplemented with 10% of fetal calf serum and 2 mM of glutamine. At 5 days, transepithelial electrical resistance (TER) and paracellular tracer flux were measured. TER was measured using Milicell ERS (Millipore). The mean blank value, which was derived from the electrical resistance of Transwell filters without cells, was subtracted from electrical resistance. TER was determined by multiplying the electroresistance by the area of the Transwell filter. To measure the paracellular tracer flux, the medium of the upper chamber was replaced with a medium containing 200 μM fluorescein, and the cells were incubated for 1 h at 37°C. The medium of the lower chamber was collected, and fluorescent intensity was measured with a microplate reader (SpectraMax Paradigm, Molecular Devices). The fluorescent intensity of the medium lacking fluorescein acted as a blank. The mean

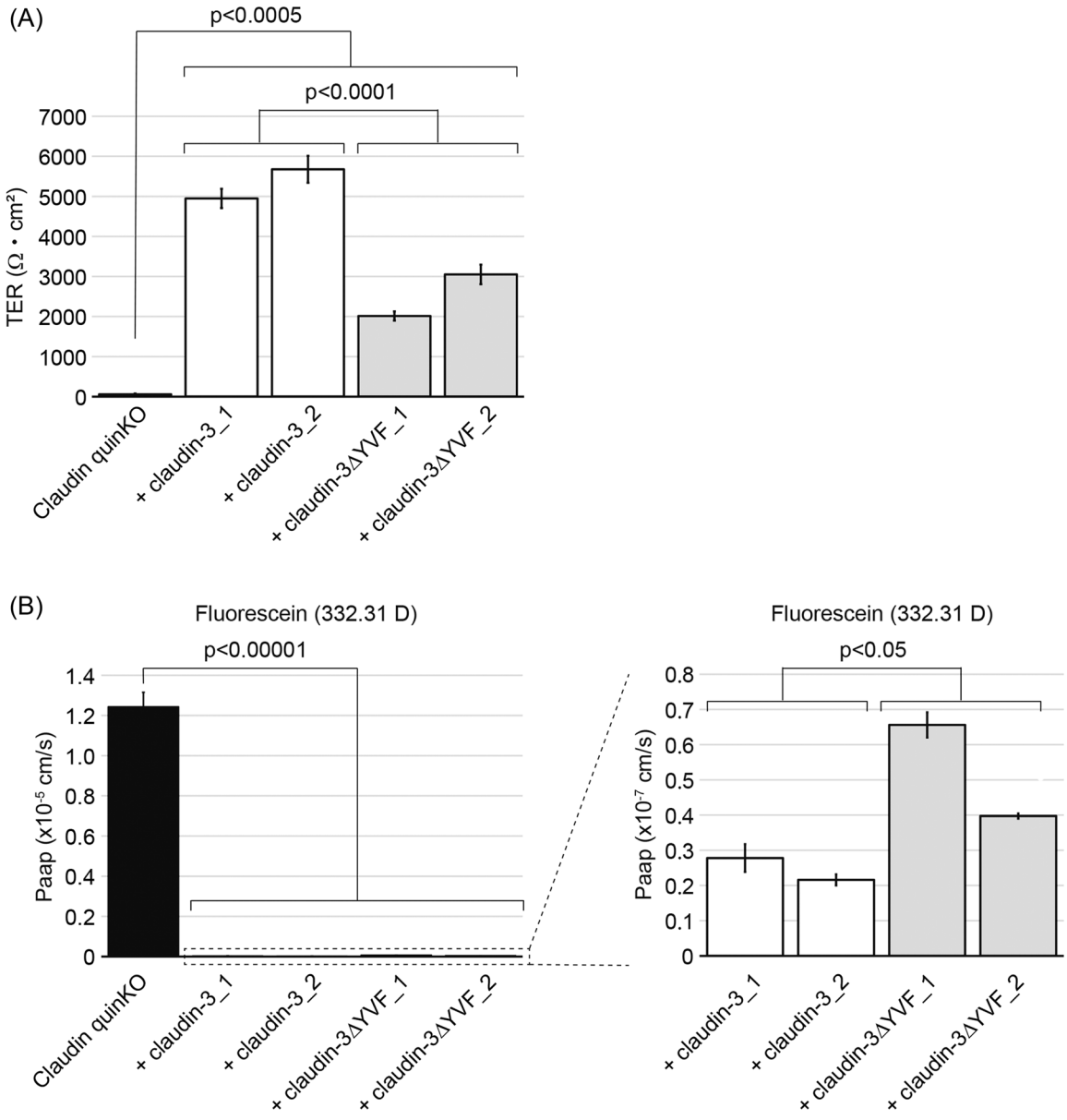

FIGURE 4 Epithelial barrier function of claudin-3- and claudin-3ΔYVF-expressing cells. (A) TER measurements of claudin quinKO cells, claudin-3-expressing cells, and claudin-3ΔYVF-expressing cells. Expression of claudin-3 or claudin-3ΔYVF increased the TER value. The effect of claudin-3 was greater compared to claudin-3ΔYVF. $N = 3$ each, unpaired, two-tailed *t*-test. (B) The paracellular flux of fluorescein in claudin quinKO cells, claudin-3-expressing cells, and claudin-3ΔYVF-expressing cells. Expression of claudin-3 or claudin-3ΔYVF reduced the paracellular diffusion of fluorescein. The effect of claudin-3 was greater compared to claudin-3ΔYVF. The right panel is an enlargement of the dotted box region in the left graph. $N = 3$ each, unpaired, two-tailed *t*-test.

blank fluorescence was subtracted from the fluorescent intensities of the samples. Apparent permeability (Papp) was calculated using the following equation: Papp = (dQ/dt)/ACo (dQ is the amount of tracer transported to the basal chamber; dt is incubation time; A is the area of the Transwell filters; and Co is initial concentration of tracer in the apical chamber). Papp calculation, statistical analyses (unpaired two-tailed *t*-test, $p < 0.05$ was set to indicate significance), and plot generations were performed using Excel (Microsoft).

Co-immunoprecipitation assay

The creation of a mammalian expression plasmid for EGFP-tagged ZO-1 (ZO-1-GFP) has been described previously.[14] Expression plasmids for NH_2-terminal HA-tagged claudin-3 and claudin-3ΔYVF were constructed by inserting each cDNA of claudin-3 and claudin-3ΔYVF into a pHA-C3 vector, which was constructed by replacing the EGFP cDNA with the HA epitope sequence in the pEGFP-C3 vector (Clontech). HEK293 cells were maintained in Dulbecco's modified Eagle's medium

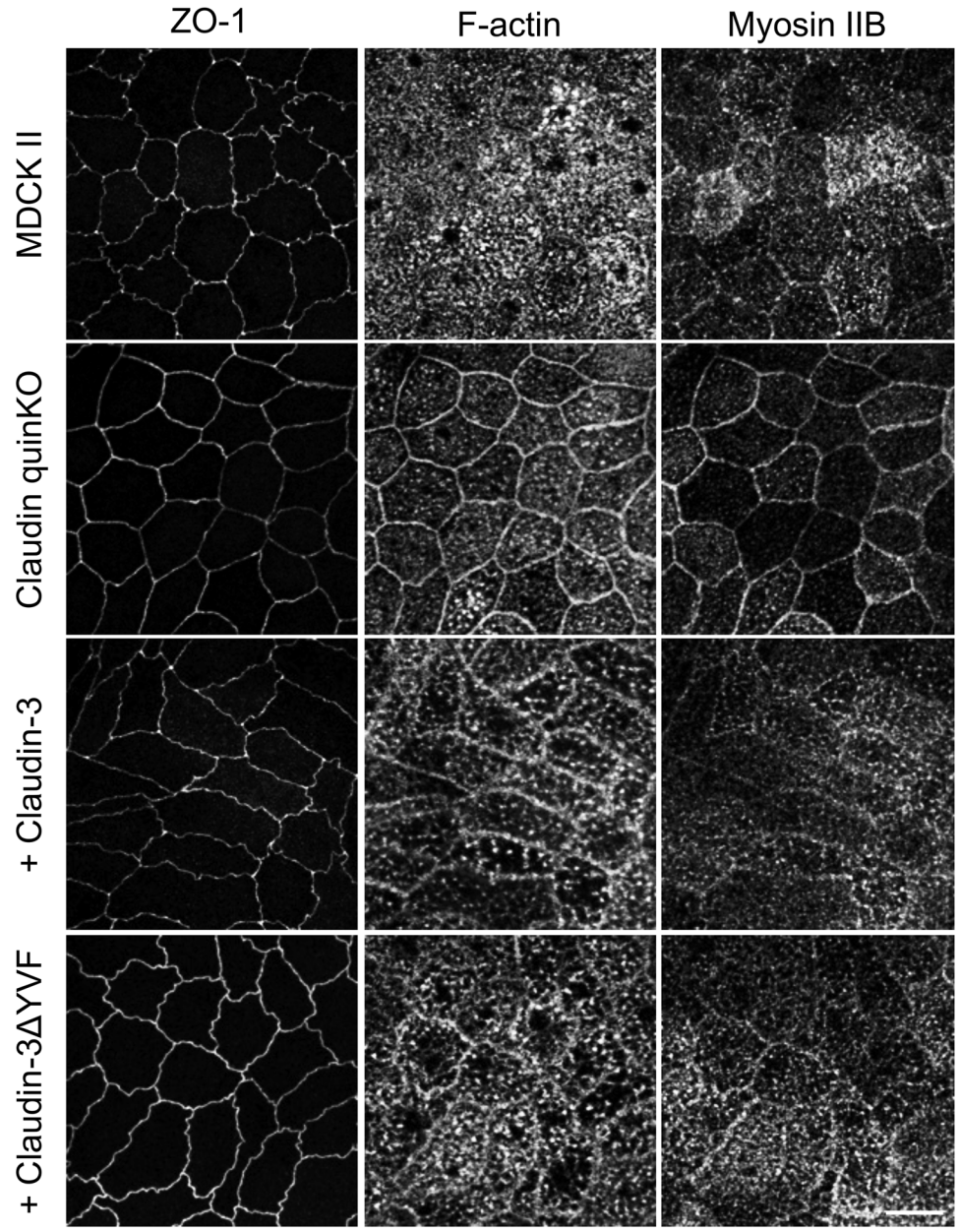

FIGURE 5 Actomyosin organization of claudin-3-expressing cells and claudin-3ΔYVF-expressing cells. Visualization of ZO-1, F-actin, and myosin IIB in MDCK II cells, claudin quinKO cells, claudin-3-expressing cells clone 2, and claudin-3ΔYVF-expressing cells clone 2. F-actin and myosin IIB were clearly concentrated at the cell junctions in claudin quinKO cells, but not in MDCK II cells, claudin-3-expressing cells, or claudin-3ΔYVF-expressing cells. Scale bar, 10 μm.

supplemented with 10% fetal calf serum and were cotransfected with ZO-1-GFP and HA-claudin-3 or HA-claudin-3ΔYVF using Avalanche Everyday Transfection Reagents (EZ Biosystems). HEK293 cells were then cultured for 2 days and lysed with ice-cold lysis buffer (50 mM Tris-HCl, pH 7.4, 150 mM NaCl, 1% NP40, 1 mM EDTA, 1 mM DTT, and a protease inhibitor cocktail [#25955; Nacalai Tesque]) and incubated on ice for 20 min. Cell lysates were clarified by centrifugation at 18,000 $\times$ *g* for 15 min and preincubated with Protein-G-Sepharose™ 4 Fast Flow (#17061801; Cytiva) for 1 h. Supernatants were incubated for 2 h at 4°C with an anti-GFP antibody and Protein-G-Sepharose™ 4 Fast Flow. Immunoprecipitates were subjected to SDS-PAGE and analyzed by immunoblotting with an anti-HA antibody.

RESULTS AND DISCUSSION

As a claudin-3 mutant lacks binding to ZO proteins, we used a construct in which the COOH-terminal tyrosine and valine were deleted, and a FLAG-tag was added (designated as claudin-3ΔYVF).[19] It was shown that the COOH-terminal tyrosine and valine of claudins are

indispensable for the binding of claudin-1 to ZO proteins.[10] Consistently, ZO-1 was colocalized with full-length claudin-1 and claudin-3 but not with those lacking the COOH-terminal tyrosine and valine at cell–cell contacts in mouse L fibroblasts.[10,19] We established two independent clones of claudin quinKO cells stably expressing claudin-3 or claudin-3ΔYVF (Figure 1A). We designated these cells as claudin-3-expressing cells and claudin-3ΔYVF-expressing cells, respectively.

Immunofluorescence staining followed by confocal microscopy of claudin-3-expressing cells revealed that claudin-3 circumscribed the cell and is concentrated at the apicolateral region of cell–cell contacts colocalizing with ZO-1 and occludin (Figure 1B). A significant amount of claudin-3 is also diffusely distributed to the lateral membrane. Two clones of claudin-3-expressing cells showed the same results (data not shown). In claudin-3ΔYVF-expressing cells, claudin-3ΔYVF was concentrated at the apicolateral region of cell–cell contacts colocalizing with ZO-1 and occludin, which is similar to claudin-3 (Figure 1B). Claudin-3ΔYVF was also diffusely distributed to the lateral membrane. Two clones of claudin-3ΔYVF-expressing cells showed the same results (data not shown).

Next, we observed TJ strands in a cell clone of each of the claudin-3-expressing or claudin-3ΔYVF-expressing cells by freeze-fracture replica electron microscopy. In claudin-3-expressing cells, a network of TJ strands was located at the most apical part of the lateral membrane as a continuous belt, consistent with immunofluorescence staining (Figure 2). In claudin-3ΔYVF-expressing cells, a network of TJ strands was reconstituted at the most apical region of the lateral membrane, which is similar to claudin-3-expressing cells (Figure 3A, A', B). However, TJ strands isolated from the apical TJ strands were often observed in the lateral membrane (Figure 3A, A', C). In addition, we found a case where a belt of apical TJ strands was discontinuous (Figure 3A', D).

Next, we examined the epithelial barrier formation of claudin-3-expressing cells and claudin-3ΔYVF-expressing cells by measuring TER and paracellular flux of fluorescein. Both claudin-3-expressing cell clones and claudin-3ΔYVF-expressing cell clones cultured on permeable filters at a confluent condition showed a remarkable increase in TER (Figure 4A) and reduction of fluorescein flux across the cellular sheet (Figure 4B). These results suggest that reconstituted TJ strands not only of claudin-3 but also of claudin-3ΔYVF in claudin quinKO cells are functional as paracellular barriers when overexpressed in claudin quinKO cells.

We reported previously that the circumferential actomyosin running along the apical cell junctions was highly developed in claudin quinKO cells.[14] To analyze the effects of the expression of claudin-3 or claudin-3 ΔYVF on actomyosin organization, we labeled ZO-1, F-actin, and myosin IIB in MDCK II cells, claudin quinKO cells, claudin-3-expressing cells, and claudin-3ΔYVF-expressing cells (Figure 5). As previously shown, the circumferential actin bundle was observed along the cell junctions with ZO-1 localization in claudin quinKO cells, while it was hardly detected in MDCK II cells. Accordingly, circumferential myosin IIB was more concentrated at the cell junctions in claudin quinKO cells than in MDCK II cells. In contrast, the signals of the circumferential F-actin and myosin IIB were weakened to just barely detectable levels not only in claudin-3-expressing cells but also in claudin-3ΔYVF-expressing cells (Figure 5). These results suggest that the actomyosin bundle formation along the cell junctions in claudin quinKO cells is not caused by the loss of claudin binding to ZO proteins, although the detailed mechanism is still unclear.

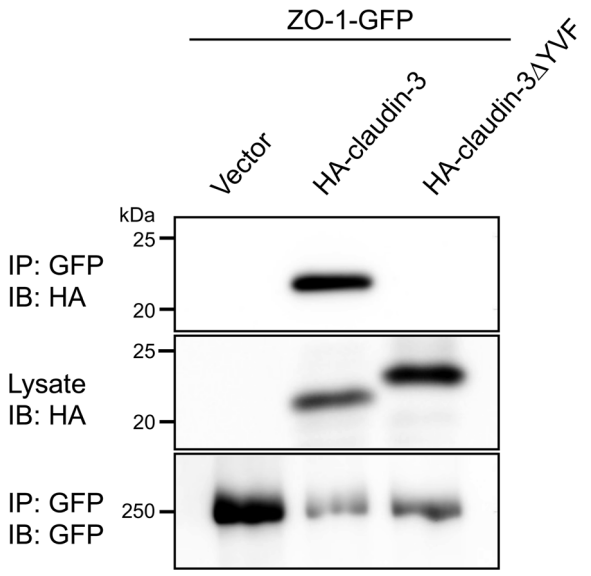

FIGURE 6 Interaction between ZO-1 and claudin-3. HEK293 cells cotransfected with ZO-1-GFP and claudin-3 or claudin-3ΔYVF were lysed and immunoprecipitated with an anti-GFP antibody. Immunoprecipitates (IP) and lysates were analyzed by immunoblotting with an anti-HA or an anti-GFP antibody. ZO-1 coprecipitated with claudin-3 but not with claudin-3ΔYVF. IB, immunoblot.

Finally, we examined whether claudin-3ΔYVF really lacks ZO-1-binding. NH_2-terminal HA-tagged claudin-3 or claudin-3ΔYVF were constructed and coexpressed with GFP-tagged ZO-1 in HEK293 cells. Cell lysates were subjected to immunoprecipitation with an anti-HA antibody, and coprecipitated ZO-1 was detected with an anti-GFP antibody in immunoblotting. As shown in Figure 6, ZO-1-GFP was coprecipitated with claudin-3 but not with claudin-3ΔYVF. These results demonstrate that claudin-3ΔYVF cannot bind to ZO-1.

Taken together, we conclude that the binding to ZO proteins is not a prerequisite for the assembly of TJ strands at the apicolateral region of cell–cell contacts. Thus, the question arises of what determines the location of TJ formation by claudin-3ΔYVF. Although claudin quinKO cells lack TJ strands, they formed JAM-A-mediated plasma membrane appositions, which circumscribed the cell at the apicolateral region.[14] These close membrane contacts by JAM-A might provide a domain for TJ formation by accelerating the trans-interaction of claudin-3. Alternatively, a certain lipid-mediated plasma membrane domain at the apicolateral region may support claudin polymerization for TJ formation. Shigetomi *et al.* found that the plasma membrane fraction purified from mouse L fibroblasts that contained claudin-1-mediated TJ strands contained a higher level of very long-chain sphingomyelin and cholesterol than that from parent L fibroblasts.[22] They also showed that the depletion of plasma membrane cholesterol in EpH4 cells by

methyl-beta-cyclodextrin treatment highly reduced the localization of claudin-3 at cell–cell contacts although other adhesion molecules, such as E-cadherin and desmoglein 2, were hardly affected.[22] It has been reported that claudins are palmitoylated, and a claudin-14, in which all four cysteine residues susceptible to palmitoylation were replaced with serine, showed less efficiency to localize at TJs when expressed in MDCK cells.[23,24] These observations support the idea that a lipid-mediated membrane domain plays a pivotal role in TJ formation. However, in this study, we did not precisely compare the protein expression level of claudin-3 and claudin-3ΔYVF in claudin quinKO cell-based stable transfectants because of the lack of an antibody that has been confirmed to recognize both constructs at equivalent affinity. Although the barrier function of claudin-3ΔYVF-expressing cells was lower than that of claudin-3-expressing cells, the difference in the ability of TJ formation between claudin-3 and claudin-3ΔYVF should be discussed based on their expression levels. To compare the efficiency to form TJs between claudin-3 and claudin-3ΔYVF in claudin quinKO cells, we need to obtain and analyze the cell clones with comparable expression levels of them using the N-terminal HA-tagged constructs in the future.

As one of the differences in reconstituted TJ strands between claudin-3-expressing cells and claudin-3ΔYVF-expressing cells, the latter contained a small gap of apical TJ strands. Since ZO proteins circumscribe the cell at the apicolateral region of cell–cell contacts, the interaction of claudins with ZO proteins may guarantee the full continuity of TJ strands along bicellular contacts. In addition, we often observed TJ strands in the lateral membrane isolated from the apical TJs in claudin-3ΔYVF-expressing cells, while these structures were not seen in claudin-3-expressing cells. This might be generated by the possibly excessive expression of claudin-3ΔYVF. Alternatively, the COOH-terminal PBM may play a role in the restriction of the location of TJ strands at the most apical part of the lateral membrane via a mechanism other than ZO proteins binding. It was shown that exogenous expression of LNX1, a ubiquitin E3 ligase containing multiple PDZ domains, bound to the PBM of claudin-1, ubiquitinated it, and reduced TJ strands in MDCK II cells.[25] It may be possible that short TJ strands are generally formed even in the lateral membrane but continuously removed by the binding to LNX1. Although it has yet to be demonstrated that the LNX1-mediated downregulation of TJs endogenously works in MDCK II cells, claudin-3ΔYVF may be escaped from this system due to the lack of its PDZ domain-binding motif.

Our results also imply that ZO proteins may regulate TJ strand formation in a manner independent of its interactions with claudins. This may involve its ability to regulate the organization of the actomyosin cytoskeleton or its ability to phase-separate to control the concentration of various molecules, which promotes the formation of a specialized plasma membrane domain that facilitates claudin recruitment. Structure-function analysis of ZO-1 to dissect the functional domains responsible for TJ strand formation may shed light on the underlying mechanisms in the future.

In conclusion, we have shown that the interaction of claudins with ZO proteins is not a prerequisite for TJ strand formation at the most apical part of cell–cell contacts, but it is needed for completely continuous TJ belts. To further clarify the role of the COOH-terminal PBM of claudins in TJ formation in more detail, we need to generate and analyze the cells expressing the full-length claudin and its mutant lacking the PBM at a comparative protein level.

ACKNOWLEDGMENTS

We thank Takako Maegawa and Hitoshi Takagi of the Life Science Innovation Center at the University of Fukui, Mika Watanabe of NIPS for their technical assistance, and Motohiro Nishida for generously allowing us to use their microplate reader. This work was supported by JSPS KAKENHI (16K15226, Grant-in-Aid for Challenging Exploratory Research to MF; 21H02523, Grants-in-Aid for Scientific Research (B) to MF; 16H06280, Grant-in-Aid for Scientific Research on Innovative Areas—Platforms for Advanced Technologies and Research Resources "Advanced Bioimaging Support" to YF).

AUTHOR CONTRIBUTIONS

M.F. conceptualized the project. M.F. conceptualized the analyses. S.F., T.P.N., K.F., Y.F., and T.O. performed the analyses. M.F. wrote the first draft of the manuscript. All authors edited the manuscript and approved the final version.

COMPETING INTERESTS

The authors have no competing interests to declare.

PEER REVIEW

The peer review history for this article is available at https://publons.com/publon/10.1111/nyas.14881.

ORCID

Mikio Furuse https://orcid.org/0000-0003-2847-8156

REFERENCES

1. Anderson, J. M., & Van Itallie, C. M. (2009). Physiology and function of the tight junction. *Cold Spring Harbor Perspectives in Biology*, *1*, a002584.
2. Otani, T., & Furuse, M. (2020). Tight junction structure and function revisited. *Trends in Cell Biology*, *30*, 805–817.
3. Shen, L. E., Weber, C. R., Raleigh, D. R., Yu, D., & Turner, J. R. (2011). Tight junction pore and leak pathways: A dynamic duo. *Annual Review of Physiology*, *73*, 283–309.
4. Zihni, C., Mills, C., Matter, K., & Balda, M. S. (2016). Tight junctions: From simple barriers to multifunctional molecular gates. *Nature Reviews Molecular Cell Biology*, *17*, 564–580.
5. Furuse, M., Sasaki, H., Fujimoto, K., & Tsukita, S. (1998). A single gene product, claudin-1 or -2, reconstitutes tight junction strands and recruits occludin in fibroblasts. *Journal of Cell Biology*, *143*, 391–401.
6. Furuse, M., Sasaki, H., & Tsukita, S. (1999). Manner of interaction of heterogeneous claudin species within and between tight junction strands. *Journal of Cell Biology*, *147*, 891–903.
7. Kubota, K., Furuse, M., Sasaki, H., Sonoda, N., Fujita, K., Nagafuchi, A., & Tsukita, S. (1999). Ca^{2+}-independent cell-adhesion activity of claudins, a family of integral membrane proteins localized at tight junctions. *Current Biology*, *9*, 1035–1038.
8. Staehelin, L. A. (1973). Further observations on the fine structure of freeze-cleaved tight junctions. *Journal of Cell Science*, *13*, 763–786.
9. Günzel, D., & Yu, A. S. L. (2013). Claudins and the modulation of tight junction permeability. *Physiological Reviews*, *93*, 525–569.

10. Itoh, M., Furuse, M., Morita, K., Kubota, K., Saitou, M., & Tsukita, S. (1999). Direct binding of three tight junction-associated MAGUKs, ZO-1, ZO-2, and ZO-3, with the COOH termini of claudins. *Journal of Cell Biology*, *147*, 1351–1363.
11. Fanning, A. S., & Anderson, J. M. (2009). Zonula occludens-1 and -2 are cytosolic scaffolds that regulate the assembly of cellular junctions. *Annals of the New York Academy of Sciences*, *1165*, 113–120.
12. Farquhar, M. G., & Palade, G. E. (1963). Junctional complexes in various epithelia. *Journal of Cell Biology*, *17*, 375–412.
13. Umeda, K., Ikenouchi, J., Katahira-Tayama, S., Furuse, K., Sasaki, H., Nakayama, M., Matsui, T., Tsukita, S., Furuse, M., & Tsukita, S. (2006). ZO-1 and ZO-2 independently determine where claudins are polymerized in tight-junction strand formation. *Cell*, *126*, 741–754.
14. Otani, T., Nguyen, T. P., Tokuda, S., Sugihara, K., Sugawara, T., Furuse, K., Miura, T., Ebnet, K., & Furuse, M. (2019). Claudins and JAM-A coordinately regulate tight junction formation and epithelial polarity. *Journal of Cell Biology*, *218*, 3372–3396.
15. Furuse, M., Fujita, K., Hiiragi, T., Fujimoto, K., & Tsukita, S. (1998). Claudin-1 and -2: Novel integral membrane proteins localizing at tight junctions with no sequence similarity to occludin. *Journal of Cell Biology*, *141*, 1539–1550.
16. Saitou, M., Ando-Akatsuka, Y., Itoh, M., Furuse, M., Inazawa, J., Fujimoto, K., & Tsukita, S. (1997). Mammalian occludin in epithelial cells: Its expression and subcellular distribution. *European Journal of Cell Biology*, *73*, 222–231.
17. Itoh, M., Yonemura, S., Nagafuchi, A., Tsukita, S., & Tsukita, S. (1991). A 220-kD undercoat-constitutive protein: Its specific localization at cadherin-based cell–cell adhesion sites. *Journal of Cell Biology*, *115*, 1449–1462.
18. Stevenson, B. R., Siliciano, J. D., Mooseker, M. S., & Goodenough, D. A. (1986). Identification of ZO-1: A high molecular weight polypeptide associated with the tight junction (zonula occludens) in a variety of epithelia. *Journal of Cell Biology*, *103*, 755–766.
19. Ikenouchi, J., Sasaki, H., Tsukita, S., Furuse, M., & Tsukita, S. (2008). Loss of occludin affects tricellular localization of tricellulin. *Molecular Biology of the Cell*, *19*, 4687–4693.
20. Hayashi, K., Yonemura, S., Matsui, T., & Tsukita, S. (1999). Immunofluorescence detection of ezrin/radixin/moesin (ERM) proteins with their carboxyl-terminal threonine phosphorylated in cultured cells and tissues. Application of a novel fixation protocol using trichloroacetic acid (TCA) as a fixative. *Journal of Cell Science*, *112*, 1149–1158.
21. Saito, A. C., Higashi, T., Fukazawa, Y., Otani, T., Tauchi, M., Higashi, A. Y., Furuse, M., & Chiba, H. (2021). Occludin and tricellulin facilitate formation of anastomosing tight-junction strand network to improve barrier function. *Molecular Biology of the Cell*, *32*, 722–738.
22. Shigetomi, K., Ono, Y., Inai, T., & Ikenouchi, J. (2018). Adherens junctions influence tight junction formation via changes in membrane lipid composition. *Journal of Cell Biology*, *217*, 2373–2381.
23. Rodenburg, R. N. P., Snijder, J., Van De Waterbeemd, M., Schouten, A., Granneman, J., Heck, A. J. R., & Gros, P. (2017). Stochastic palmitoylation of accessible cysteines in membrane proteins revealed by native mass spectrometry. *Nature Communication*, *8*, 1280.
24. Van Itallie, C. M., Gambling, T. M., Carson, J. L., & Anderson, J. M. (2005). Palmitoylation of claudins is required for efficient tight-junction localization. *Journal of Cell Science*, *118*, 1427–1436.
25. Takahashi, S., Iwamoto, N., Sasaki, H., Ohashi, M., Oda, Y., Tsukita, S., & Furuse, M. (2009). The E3 ubiquitin ligase LNX1p80 promotes the removal of claudins from tight junctions in MDCK cells. *Journal of Cell Science*, *122*, 985–994.

How to cite this article: Fujiwara, S., Nguyen, T. P., Furuse, K., Fukazawa, Y., Otani, T., & Furuse, M. (2022). Tight junction formation by a claudin mutant lacking the COOH-terminal PDZ domain-binding motif. *Ann NY Acad Sci.*, *1516*, 85–94. https://doi.org/10.1111/nyas.14881